Screening of Iberian coinage in the 2th-1th BCE period using the voltammetry of immobilized particles

Antonio Doménech-Carbó*[a], María Teresa Doménech-Carbó[b], Carla Álvarez-Romero[b], Trinidad Pasíes[c], Milagros Buendía[d]

[a] Departament de Química Analítica. Universitat de València. Dr. Moliner, 50, 46100 Burjassot (València) Spain.

[b] Institut de Restauració del Patrimoni, Universitat Politècnica de València, Camí de Vera 14, 46022, València, Spain.

[c] Museu de Prehistòria de València. Corona 36, 46003, Valencia, Spain.

[d] Museo Nacional de Arqueología Subacuática, Cartagena, Spain.

* Corresponding author; e-mail: antonio.domenech@uv.es

Abstract

The voltammetry of immobilized particles (VIMP) was applied for grouping a series of 86 Iberian coins nominally minted in the cities of Iltirta, Cástulo and Obulco in the 2th-1th BCE period for which there are no chronological data. Using characteristic signatures for the reduction of cuprite, tenorite and lead corrosion products in the patina of the coins, voltammetric grouping of coins was proposed. Voltammetric data were found to be consistent with textural and compositional properties of the surface and subsurface of selected coins using FIB-FESEM-EDX. The obtained data confirmed a clear separation between the productions of Iltirta on one side, and those of Cástulo and Obulco on the other side, indicating the possibility to establish a rough chronology for these productions.

Keywords: Electrochemistry; Mint discrimination; Iberian coins; Iltirta; Cástulo; Obulco.

Introduction

Although the earliest Iberian Peninsula coinage started at the end of the 6th century BCE, extensive minting and circulation began at the end of the 3rd century BCE, during the Second Punic War, and was prolonged until the mid-first century AD. Iberian currency consisted on civic coinages produced by individual cities and were progressively replaced by imperial coinages [1,2].

The civic Iberian coins have attracted considerable attention because of being one of the more important material supports for establishing provenance of raw materials and economical and political linkages between cities and their relationships with the Romans. The historical and archaeological studies, however, are complicated by the absence of a minting chronology (Iberian coins do not have emission dates) and the abundance of forgeries [1,2].

In this context, analytical techniques play an essential role for achieving the information demanded by archaeologists and historians. The basic information is derived from the knowledge of the composition and metallographic structure of the coins [3,4] spectroscopic and diffraction techniques [5-10], and isotope analysis [11,12]. One important problem is the existence of a more or less extensive corrosion of the coins, so that invasive sampling is needed to reach the metal core. For obvious reasons of conservation of the integrity of the studied coins, the practice of several analytical methods are limited to archaeological objects satisfying very specific conditions [13,14]. Accordingly, there is an increasing interest in the application of non-invasive or minimally invasive techniques aimed to extract analytical information from the metal patina [15-18].

In the last decade, the voltammetry of immobilized particles (VIMP), a solid-state electrochemical methodology developed by Scholz et al. [19,20] for characterizing sparingly soluble solids, has been applied to cultural heritage and, in particular, to the study of archaeological metals [21-24]. Only requiring sample amounts at the sub-microgram level, the VIMP has been applied for identifying metals and their corrosion products [25-31] as well as, via optimized sampling strategies [32,33], for local analysis of corrosion layers [34,35], authentication [36,37] and dating [38-41] of different archaeological metals.

This methodology, as well as all other techniques based on the patina analysis, has one significant inherent difficulty: the composition and layered structure of the metal patinas depend not only on the composition and metallography of the base metal but also on the 'corrosion history' experienced by the object. In spite of this difficulty, there is the possibility to acquire analytical information of archaeometric interest in series of samples for which it is possible to assume a common or quite similar corrosion history and directing the sampling to regions of the objects presenting homogeneous patination. Under these restricting conditions, previous studies on ten-cash coins from the last Chinese emperors [42] and Spanish *maravedís* minted between 1661 and 1664 [43], and Roman bronze coins from the Magna Mater temple [44] permitted to establish electrochemical criteria for discriminating between different monetary emissions.

Here, we report a VIMP study on a series of bronze coins ascribed to three Iberian mints: Iltirta, Cástulo, and Obulco, all corresponding to an undefined period between the 2th and the 1th century BCE. The production of the first city, located near the Ebro valley (north-east of the Iberian Peninsula) consisted mainly of ternary Cu-Sn-Pb alloys [1,2,45-47]. In contrast, Cástulo and Obulco, located in the vicinity of the Guadalquivir valley (South of the Iberian Peninsula), and consequently far from the sources of cassiterite at the north-west of the Iberian Peninsula [48], produced Sn-free coins and their production was more irregular than that of Iltirta [45-47].

2. Experimental

2.1. Samples

Three sets of coins extracted in different archaeological sites ascribed to the mints of Iltirta (18 coins), Cástulo (47 coins), and Obulco (21 coins) from the Museu de Prehistòria de València were studied. Their description is presented in Supplementary Information, Table S.1. The studied coins were selected as those presenting regions of uniform corrosion and the absence of localized aggregates of green corrosion products. It is pertinent to note that there is possibility of some natural or anthropogenic accumulation of lead and other components onto the coins surface, thus distorting the representativity of data. The disposal, for each mint, of a relatively high number of

coins from different archaeological provenances permits to some extent a compensation of this biasing effect although it may result in the increase of dispersion of voltammetric data for each production center. Sampling was performed by pressing and lightly rotating onto such regions a commercial paraffin-impregnated graphite bar (pencil leads: Faber Castell, HB type, 2.0 mm diameter) during ca. 5 seconds. One-three replicate measurements were carried out for each coin sampling in different regions of apparently equivalent patination. To avoid 'memory' effects, the voltammetric measurements were performed after randomized distribution of the coins. Although repeated sampling on the same region could be used for obtaining layer-by-layer information [35], this was not performed to avoid possible contamination and facilitate the subsequent coin cleaning, easily made with an acetone-impregnated cotton bar.

2.2. Instrumentation and methods

Electrochemical experiments were performed at 298 K in a three-electrode cell using air-saturated aqueous 0.25 M sodium acetate buffer (Panreac) at pH 4.75 as a supporting electrolyte. No deaeration of the electrolyte was carried out in order to mimic the conditions for applying this methodology in field, a practice that does no distort significantly the voltammetric response of the metal corrosion products under our experimental conditions (vide infra). To avoid possible contamination by metal ions released during voltammetric cycles, the electrolyte was renewed after each electrochemical run. Voltammograms were recorded using a CH I660C potentiostat (Cambria Scientific, Llwynhendy, Llanelli UK) and completing the three-electrode arrangement with a platinum wire auxiliary electrode and an Ag/AgCl (3 M NaCl) reference electrode. For each coin, samples were taken by abrasively pressing onto 1-3 different regions of the coins showing a dark brown uniform hue, as already described [43,44].

VIMP for reference materials was carried out using conventional VIMP protocols [19,20] by powdering an amount of 1-2 mg of the solid in an agate mortar and pestle, and extending it on the agate mortar forming a spot of finely distributed material. Then the lower end of the graphite electrode was gently rubbed over that spot of sample and finally rinsed with water to remove ill-adhered particles. Sample-modified graphite bars

were then dipped into the electrochemical cell so that only the lower end of the electrode was in contact with the electrolyte solution.

The microstructure of coins was determined using field emission scanning electron microscopy (Model S-4800, Hitachi Ltd., Tokyo, Japan) operating at 20 kV. The microanalysis of samples was performed with a X-ray microanalysis system (SEM/EDX). Photographic images of coins were carried out with a Leica M165 stereo microscope using a capture system of high resolution digital image IC80HD controlled by LAS program. Sectioning and imaging of the coins was performed with a FIB-FESEM Zeiss (Orsay Physics Kleindiek Oxford Instruments) model Auriga compact equipment that enabled the characterization of the microtexture and mineral phases in the superficial corrosion layer and in the metal core. The operating conditions were: voltage, 30 kV and current intensity, 500µA and 20 nA in the FIB for generating the focused beam of Ga ions and a voltage of 3 kV in the FESEM.

3. Results and discussion

3.1. Voltammetric pattern

Figure 1 shows the square-wave voltammograms of samples of coins (a,b) 41593 from Obulco and (c,d) 41540 from Cástulo, attached to graphite electrodes immersed into air-saturated 0.25 M HAc/NaAc at pH 4.75. Upon scanning the potential from 0.65 V vs. Ag/AgCl in the negative direction (Fig. 1a,c), cathodic peaks appear at –0.10 (C_1), –0.40 (C_2) and –0.55 (C_3). When the potential is scanned from –1.05 V in the positive direction, anodic signals at –0.45 (A_2) and 0.05 V (A_1) appear, frequently displaying peak splitting. Since no electrolyte deoxygenation was performed, the above signals are accompanied by a cathodic shoulder at –0.70 (C_{ox}) corresponding to the reduction of dissolved oxygen. Under our experimental conditions, this process does not interfere significantly in the voltammetric response of the components of the metal patina, as denoted by blank experiments in deaerated solutions.

This voltammetry is in agreement with previous data of archaeological copper and bronze [34,35,39,42,43] and leaded bronzes [40,44] and can be rationalized by

considering voltammograms for reference corrosion products and their mixtures. As can be seen in Figure 2, in which the voltammograms of microparticulate deposits of mixtures of a) cuprite plus tenorite, b) cuprite plus litharge, and c) cuprite plus tenorite plus litharge, are depicted. Cuprite (Cu_2O) usually forms the primary patina of copper/bronze objects further forming a secondary patina where it is accompanied by other copper corrosion products depending on the environment [17,18]. This compound is responsible for the cathodic wave C_1 while the peak C_2 is attributable to tenorite (CuO). This signal is overlapped with the peak C_3, which can be assigned to lead corrosion products, usually litharge (PbO) whose porous forms are reduced at potentials at ca. –0.90 V [36-38,49,50]. Increasing the proportion of PbO results in the merging of signals C_2 and C_3. The above reduction processes yield different deposits of Cu and Pb metal which are oxidized to the corresponding M^{2+} (M = Cu, Pb) ions in solution during the stripping processes A_1, A_2. In general, signals attributable to Sn and Zn compounds are not obtained because, due to the extended process of destannification and dezincication, these metals are not anymore present [17,18,51,52].

The net amount of sample extracted in each voltammetric experiment can be estimated from the charge passed calculated using the area under the voltammetric peaks. Taking for this purpose the stripping peaks (see Figs. 1b,d) for Cu and Pb, we obtained charge amounts between 1 and 10 μC which correspond, roughly, to Cu or Pb amounts between 1 and 10 ng.

Figure 3 depicts a possible scheme of the structure of the corrosion patina of binary (Cu-Sn) and ternary (Cu-Sn-Pb) bronzes in the absence of gross corrosion yielding corrosion products of the hydroxycarbonate, hydroxysulfate and hydroxichloride families. In the first case, in principle equivalent to copper, there would be a primary patina of ‘impermeable’ oxygen-defective cuprite [28,53-55] accompanied by a ‘porous’ secondary patina progressively enriched in tenorite. Accordingly, one can expect an increase of the ratio between the intensities of the signals C_2 and C_1 from deeper to surface layers [42-44].

In the case of ternary alloys, given the known low solubility of lead into copper results, there is a formation of characteristic peculiar globular features of lead and corrosion patterns [51,56,57], one can assume that litharge forms separate primary and secondary

deposits between the copper corrosion layers. As a result, one can expect that the ratio between the intensity of the signals C_3 and C_1 (and/or C_2) would be representative of the composition –but also on the metallurgical manufacturing- of the base alloy. Due to the in principle larger corrosivity of lead relative to copper, the ratio between the peak currents of C_3 and C_1 (and/or C_3 andC_2) should be larger than the averaged Pb/Cu ratio in the base metal. The same consideration applies for the ratio between the peak currents of the oxidative dissolution process A_2 (stripping of Pb) and A_1 (stripping of Cu). On first examination, this ratio, $i_p(A_2)/i_p(A_1)$, can be considered as proportional to the average Pb/Cu molar ratio in the corrosion layers and, ultimately, proportional (or to some extent representative) of the average Pb/Cu molar ratio in the base metal alloy.

3.2. Correlation with compositional data

In order to evaluate the precedent hypotheses, voltammetric data were compared with data of elemental composition reported in literature [45-47] for Iberian coins. Since such data correspond to sets of coins different from those studied here, there is no possibility of direct data correlation. However, some global, indirect comparative analysis is possible.

Compositional data of the bulk metal alloy reported by Ripollés et al. [45-47] for coins of Iltirta, Ilerda (the Imperial continuation of the Republican Iltirta), Cástulo and Obulco are presented as Supplementary Information, Table S.2. As can be seen in Figure 4a, where a two-dimensional diagram containing the mass percentages of Cu and Pb is depicted, the coins of Iltirta, Cástulo and Obulco can be grouped into three separate tendency curves, excluding two 'anomalous' coins from Cástulo, marked by arrows. Overall, this graph can be interpreted in terms of a growing use of lead in the order Iltirta < Cástulo < Obulco, coincident with that expected due to the proximity of the southern cities to the sources of lead minerals [45-47]. A more refined separation can be established on considering the percentage of tin, which is plotted as a function of the percentage of lead in double logarithmic scale in Figure 4b. Here, one can see that the Iltirta coins possess Sn percentages around 4 wt-%, while all Obulco and Cástulo coins with several exceptions (marked by arrows) possess percentages of Sn below the 1 wt-%.

Accordingly, there is a frontier between Iltirta coins, characterized by high Sn loadings, resulting from the deliberate addition of tin minerals, and Cástulo and Obulco coins, where the proportion of this metal is below 1 wt-%, attributable to the trace Sn accompanying Cu and Pb minerals rather than a deliberate addition, a logical feature giving the previously indicated separation of these cities from the cassiterite mines in the north-west of the Iberian Peninsula [48]. Interestingly, the Iltirta coins appear to be separated into two groups (A and B) with clearly different Pb loadings. This feature will be further treated in relation to electrochemical data.

In this context, the presence of 'anomalous' coins from Cástulo and Obulco having high Sn loadings can be interpreted as a result of reusing metal from secondary sources.

Figure 5 depicts the variation of the ratio between the peak current of the processes C_2 and C_1, $i_p(C_2)/i_p(C_1)$, on the peak current of the process C_1 for the Iberian coins in this study. One can see that the data points for Iltirta coins fall in a region of the diagram clearly separated from those of Cástulo and Obulco, with the exception of one or two coins from these mints. Taking into account that, roughly, these signals are representative of the averaged amount of copper and lead compounds in the corrosion layers (vide infra), three aspects can be underlined:

a) Voltammetric data permits to discriminate the production of Iltirta from those of Cástulo and Obulco mints and, to a lesser extent, between these last two cities.
b) There are (few) anomalous coins from Cástulo and Obulco, in agreement with compositional data.
c) The Pb content in the corrosion layers of the Iltirta coins is lower than that in Cástulo and Obulco coins, in agreement with compositional data reported by Ripollés et al. [45-47].

The feature c) is in apparent contrast to composition data from Ripollés et al. on the metal composition of Iberian (a different set of) coins from the same mints. This apparent discrepancy can be interpreted as the result of the differences in the base metal, in particular, by the relatively high presence of Sn in the Iltirta coins. Since Sn is efficiently removed from the corrosion layers (the well-known destannification phenomenon [17,18,51,52]), it exerts a more efficient sacrificial role than Pb; i.e., the

rate of Cu corrosion relative to Pb is lowered in Iltirta coins relative to Cástulo and Obulco ones.

3.3. Modeling depth variation of voltammetric and compositional parameters

As described in previous reports [42-44], the sampling for VIMP measurements implies the transference of different amounts at the level of few nanograms of materials from the corrosion layers of the coins so that the average composition of the sample depends on the depth reached during the process. The measured currents for the different processes can be taken as proportional to the net amount of the materials responsible of that process. Then, one can assume that the peak current of the process C_1, $i_p(C_1)$; is representative of the net amount of cuprite, m_{cup}, transferred to the graphite electrode,

$$i_p(C_1) = g_{cup} m_{cup} \qquad (1)$$

whereas the peak C_2, $i_p(C_2)$; will be representative of the contributions of tenorite and litharge (m_{ten}, m_{lit}). Then:

$$i_p(C_2) = g_{ten} m_{ten} + g_{lit} m_{lit} \qquad (2)$$

In the above equations, g_{cup}, g_{ten}, g_{lit}, denote the respective coefficients of electrochemical response dependent on the fixed experimental conditions (scan rate, etc.). In turn, the peak current of anodic signals A_1 and A_2 ($i_p(A_1)$, $i_p(A_2)$) will be representative of the total amount of copper corrosion products and lead corrosion products, respectively. Then, introducing the corresponding coefficients of electrochemical response one can write:

$$i_p(A_1) = g_{Cu}(m_{cup} + m_{ten}) \qquad (3)$$

$$i_p(A_2) = g_{Pb} m_{lit} \qquad (4)$$

Combining Eqs. (1) and (3), the tenorite to cuprite ratio in a given measurement is as follows:

$$\frac{m_{ten}}{m_{cup}} = \frac{1 - \left(\frac{g_{Cu}}{g_{cup}}\right)\left(\frac{i_p(C_1)}{i_p(A_1)}\right)}{\left(\frac{g_{Cu}}{g_{cup}}\right)\left(\frac{i_p(C_1)}{i_p(A_1)}\right)} \qquad (5)$$

This is an average value for the portion of patina submitted to sampling; i.e. the m_{ten}/m_{cup} ratio varies from one voltammetric experiment to another. In order to account for the differences in the amount of transferred sample between different experiments, it is assumed that in each sampling, a volume V of corrosion products corresponds to a cylinder of surface S and height x. Here, the number of tenorite grains per volume unit, n_{ten}, increases from zero in the primary/secondary patina boundary ($x = \delta$) to a value n_{ten}^{sup} at the external surface of the secondary patina ($z = 0$) while the number of cuprite grains per volume unit, n_{cup}, decreases from its value in the primary patina, n_{cup}^{o}, to the value reached at the external surface, n_{cup}^{sup}. If the concentration gradients of cuprite and tenorite are given by potential functions expressed in terms of a normalized depth $z = 1 - x/\delta$ [42-44]:

$$m_{cup} = \int_0^z S[n_{cup}^{o} - n_{ten}^{sup} z^{\alpha}]dz = S[n_{cup}^{o} - \frac{n_{ten}^{sup} z^{1+\alpha}}{1+\alpha}] \qquad (6)$$

$$m_{ten} = \int_0^z S n_{ten}^{sup} z^{\alpha} dz = \frac{S n_{ten}^{sup} z^{1+\alpha}}{1+\alpha} \qquad (7)$$

Applying similar considerations for the case of litharge, its concentration in the secondary patina increases from the value in the primary patina, n_{lit}^{o}, to the value reached at the external surface, n_{lit}^{sup} as:

$$m_{lit} = \int_0^z S[n_{lit}^{o} + n_{lit}^{sup} z^{\beta}]dz = S[n_{lit}^{o} + \frac{n_{lit}^{sup} z^{1+\beta}}{1+\beta}] \qquad (8)$$

This means that the ratio between the peak currents of A_1 and A_2 will be dependent on the depth reached in the sampling process as:

$$\frac{i_p(A_2)}{i_p(A_1)} = \frac{g_{lit}\left[n^o_{lit} + \frac{n^{sup}_{lit} z^{1+\beta}}{1+\beta}\right]}{g_{ten}\frac{n^{sup}_{ten} z^{1+\alpha}}{1+\alpha} + g_{cup}\left[n^o_{cup} - \frac{n^{sup}_{cup} z^{1+\alpha}}{1+\alpha}\right]} \qquad (9)$$

After testing different pairs of parameters, the more clear discrimination between mints was obtained using the peak currents of the lead-centered process C_2 and A_2. As shown in Figure 6, plots of $i_p(C_2)$ vs. $i_p(A_2)$ provide again a rough discrimination between the three mints. For grouping purposes within each city, the ratio between the peak currents of C_1 and C_2, which is dependent on both Cu-centered and Pb-centered electrochemistry were used. The ratio between the corresponding peak currents is:

$$\frac{i_p(C_1)}{i_p(C_2)} = \frac{g_{cup}\left[n^o_{cup} - \frac{n^{sup}_{cup} z^{1+\alpha}}{1+\alpha}\right]}{g_{ten}\frac{n^{sup}_{ten} z^{1+\alpha}}{1+\alpha} + g_{lit}\left[n^o_{lit} + \frac{n^{sup}_{lit} z^{1+\beta}}{1+\beta}\right]} \qquad (10)$$

Since blank experiments such as in Figure 2 denote that $g_{lit} >> g_{cup}$, g_{ten}, one can approximate $i_p(C_2) \approx g_{lit} n^{sup}_{lit} z^{1+\beta}/(1+\beta) >> g_{lit} n^o_{lit}$ and assuming $\alpha \approx \beta$, one can approximate:

$$\frac{i_p(C_1)}{i_p(C_2)} = \frac{g_{cup}\left[n^o_{cup} - \left(\frac{i_p(C_2)}{g_{lit} n^{sup}_{lit}}\right)\right]}{i_p(C_2)\left[1 + \left(\frac{g_{ten}}{g_{lit}}\right) i_p(C_2)\right]} \qquad (11)$$

This equation predicts a polynomial variation of the $i_p(C_1)/i_p(C_2)$ ratio on $i_p(C_2)$ depending on the electrochemical parameters and the coin-sensitive parameters n^o_{cup}, n^{sup}_{lit}. Experimental data (see section 3.5 below) for the studied coins are in agreement with this prediction.

3.4. FESEM-FIB data

Figure 7 depicts the secondary electron images recorded in trenches of *ca.* 10 μm length and *ca.* 15 μm depth in FESEM-FIB examination of coins a) 42127 (Iltirta); b) 41868 (Iltirta); c) 25654 (Cástulo); d) 25671 (Obulco). One can see that coins 42127 and

25671 present an inner, metallic region consisting of 1-2 μm-sized domains intercalated into an apparently continuous matrix. For these coins the EDX elemental analysis provided averaged percentages of Cu between 90-95 wt-% without Pb and Sn content below 1 wt-%. In contrast, the Iltirta coin 41868 displayed an apparently uniform porous structure with a high Sn content (larger than 30 wt-%) and a Pb content up to 5 wt-%. Both the textural and compositional properties differ clearly from the Iltirta coin 42127, thus suggesting that there were at least two different production types in this mint. Finally, Obulco coin 25671 produced a gross division into two uniform textures suggesting the presence of Pb accumulations, as evidenced by the averaged composition where Sn was absent but the Pb content reached ca. 34 wt-%. These data, which are qualitatively in agreement with previous studies on coins from different historical periods [42-44], indicate that there are relevant differences in the composition and microtexture of the corrosion layer in the upper region of the trench, in turn reflecting the differences in minting.

3.5. Grouping

The first insight derived from the voltammetric data is that the set of coins from Cástulo and Obulco were more heterogeneous than the Iltirta set. This can be clearly seen in Figure 8, in which the distribution of frequencies of the $i_p(A_2)/i_p(A_1)$ ratio values for a) Iltirta and b) Cástulo plus Obulco coins in this study are depicted separately. This is entirely consistent with historic and archaeological data: the Iltirta minting was an official controlled production, whereas official coin productions from Cástulo and Obulco were accompanied by numerous imitations/falsifications in other mints of the same region [45-47].

In order to extract archaeometric information from the above VIMP data it has to be taken into account that for coins of the copper and binary bronze having and similar corrosion history, the tenorite/cuprite ratio should increase with age [39] whereas for leaded bronzes, the proportion of lead corrosion products to copper corrosion products increases with age [40]. Since the data presented in precedent sections indicate that the last ratio is sensitive to the Sn loading in ternary bronzes, grouping of coins was in principle made separately for Iltirta (ternary bronzes) and Cástulo plus Obulco (binary bronzes) using the $i_p(C_1)/i_p(C_2)$ vs. $i_p(C_2)$ curves.

Figure 9 shows the $i_p(C_2)/i_p(C_1)$ vs. $i_p(C_1)$ plots for coins from the Iltirta mint in this study. One can see in this figure that the experimental data points can be fitted to three tendency lines consistent with the theoretical prediction from Eq. (11). This graph permits to divide the Iltirta coins in three groups (I-1 to I-3) in principle corresponding to increasing lead corrosion products plus tenorite to cuprite ratio. As previously noted, upon assuming uniform conditions of corrosion, this increase can be attributed to both the increase in the Pb content in the base metal alloy (and/or a concomitant decrease in the Sn coontent) and the increase in the corrosion time. Since the time interval in which the mint was operative was of ca. 200 years [45-47], it appears that the variations in the Pb content of the coins was the main effect to be accounted. Accordingly, one can hypothesize that the production of the Iltirta mint occurred in (at least) three different steps.

Figure 10 presents the $i_p(C_2)/i_p(C_1)$ vs. $i_p(C_1)$ graph of the coins of Cástulo and Obulco incorporating the tendency lines for the I-1, I-2 and I-3 Iltirta types. Here, one can remark that practically all Cástulo and Obulco data points fall below the I-3 tendency curve. This means that the Pb content of the coins minted in these cities was Pb-enriched relative to the coinage from Iltirta, in agreement with compositional data in literature [45-47]. Although the dispersion of data does not allow for a clear discrimination of series, two extreme groups of Cástulo and Obulco coins can be discerned: one clearly defining a tendency curve close to that of the Iltirta series I-3, labeled as CO-1, and other defining the lower limiting curve (i.e., the major Pb content). This series is labeled as CO-3 while the data points intermediate between the extreme series will be labeled as CO-2. Remarkably, the Obulco coins dominate clearly the series CO-1 while the series CO-3 is formed by Cástulo coins with except one coin from Obulco.

This grouping can be in principle interpreted as resulting from two possible scenarios: a) as the result of the application of different coin productions in each center without a definite chronology, and, b) as corresponding to successive productions during the 2th – 1th BCE time interval.

Unfortunately, the absence of detailed historical data, makes highly speculative the association of composition data and electrochemical features with the scarce information existing on the involved period in which the more relevant events took place, apparently, the alignment of Iltirta with Carthago in 218 BCE and its Roman conquet in 206 BCE. In this context, it is possible to draw an (highly) hypothetical picture around the significance of electrochemical data in Figs. 9 and 10:

i) The series I-1 would correspond to a production of Iltirta was possibly constituted by copper or binary bronze, consistently with FIB-FESEM data for coin 42127 (see Fig. 7a) and may be an early production of the city.

ii) The series I-2 and I-3 would correspond to Iltirta productions in two successive steps now increasing the quality of the coinage via incorporating Sn and different Pb loadings. As judged by the Pb content derived from voltammetric data, and consistently with FIB-FESEM-EDX data for coin 41868 (Fig. 7b), the I-2 and I-3 productions would correspond, respectively to the 'low' and 'high' Pb contents encircled as Iltirta B and Iltirta A in Fig. 4b, respectively. Within the view b), one possible hypothesis would be the association of this production to the Roman influence.

iii) The series CO-1 would correspond to the production of Obulco (mainly) and Cástulo of higher quality, characterized by the absence of Sn and the low Pb content. Consistently, the textural properties of this type production determined in FIB-FESEM-EDX experiments with the Obulco coin 25671 (Fig. 7d). As far as it appears that the Pb content was increased with time [45-47], it appears plausible to attribute this series to the older production. Using the same line of reasoning, the CO-2 and CO-3 series to the younger emissions of Cástulo and Obulco, here superimposed to imitations fabricated in other mints of the region, for which FIB-FESEM-EDX data (Cástulo coin 25654 in Fig. 7c) reveal textural and compositional properties of copper with high Pb content.

Figure 11 depicts an interpretation of voltammetric data following the hypothetical scenario b), represented as an evolutive scheme for the monetary production in the studied cities including typical voltammograms for the different groups of coins according to their electrochemical response. Obviously, however, this picture has to be

taken with caution and further research is needed to assess the validity of this closure and the possibility of deriving a rough chronology in the Iberian coin productions.

4. Conclusions

The voltammetric response of nanosamples from a set of 86 Iberian coins from the mints of Iltirta, Cástulo and Obulco in the period 2^{th}-1^{th} BCE attached to graphite electrodes in contact with aqueous acetate buffer at pH 4.75 revealed the characteristic features of the copper (mainly cuprite and tenorite) and lead (mainly litharge) corrosion products with significant variations in the proportion of the different signals. The comparative analysis of such signals permitted to group the coin samples in terms of the relative Cu-Sn-Pb contents providing a grouping consistent with compositional and textural data extracted from the FIB-FESEM-EDX examination of several selected coins.

One of the possible hypothetical scenarios consistent with electrochemical data suggests that successive stages of monetary production occurred. According to this, the production of Iltirta would have evolved from copper to binary bronze with low or moderate Pb content in the 2^{th} – 1^{th} BCE period. As an additional hypothesis is the possibility of associate the change in coin production to the Roman influence. The production of Cástulo and Obulco, with few exceptions surely associated to the use of secondary metal sources, was dominated by copper with middle of high Pb contents, consistently with the absence of Sn raw materials and the abundance of Pb sources near to these cities and was in principle divided into three possible successive periods. Although further research is needed for assessing this evolutionary scenario, the possibility of providing a rough chronology of Iberian coin production is illustrative of the capability of the minimally invasive technique of the voltammetric of immobilized particles to yield archaeometric information complementing the scope of available methodologies in the archaeology domain.

Acknowledgements: Project CTQ2017-85317-C2-1-P, supported with *Ministerio de Economía, Industria y Competitividad* (MINECO), *Fondo Europeo de Desarrollo Regional* (ERDF) and *Agencia Estatal de Investigación* (AEI), is gratefully acknowledged. The authors wish also to thank Mr. Manuel Planes and Dr. José Luis Moya, technical supervisors of the Electron Microscopy Service of the Universitat

Politècnica de València. Thanks to Manuel Gozalbes for his technical assistance in the numismatic domain and Gonzalo Corés and the Museu de Prehistòrica de València for facilitating the access to its collections.

References

[1] P. P Ripollès, Coinage and identity in the Roman provinces: Spain, in C. J. Howgego, V. Heuchert, A Burnett, A., Eds. *Coinage and identity in the Roman provinces*, Oxford University Press, London, pp. 79–93.

[2] M. Gozalbes, Circulación y uso de los denarios ibéricos, in M., Campo, *Ús i circulació de la moneda a la Hispania Citerior*, XIII Curs d'història monetària d'Hispania, Museu de Prehistòria de València, València, pp. 83–103.

[3] D. A. Scott, *Metallography and Microstructure of Ancient and Historic Metals*, The Getty Conservation Institute, Paul Getty Museum, Malibu, 1991.

[4] I. Constantinides, M. Gritsch, A. Adriaens, H. Hutter, F. Adams, *Anal. Chim. Acta* **2001**, *440*, 189.

[5] R. Linke, M. Schreiner, *Mikrochim. Acta* **2000**, *133*, 165.

[6] M. Dowsett, A. Adriaens, *Nucl. Inst. Meth. Phys. Res. B* **2004**, *226*, 38.

[7] S. Shalev, S. Sh. Shilstein, Yu Yekutieli, *Talanta* **2006**, *70*, 909.

[8] R. Gaudiuso, M. Dell'Aglio, O. De Pascale, S. Loperfido, A. Mangone, A. De Giacomo, *Anal. Chim. Acta* **2014**, *813*, 15.

[9] J. M. del Hoyo-Meléndez, P. Swit, M. Matosz, M. Wozniak, A. Klisinska-Topacz, L. Bratasz, *Nucl. Inst. Meth. Phys. Res. B* **2015**, *349*, 6.

[10] M. Tomassetti, F. Marini, R. Bucci, L. Campanella, *Trends Anal. Chem.* **2016**, *79*, 371.

[11] P. Budd, D. Gale, A. M. Pollard, R. G. Thomas, P. A. Williams, *Archaeometry* **1993**, *35*, 241.

[12] D. Attanasio, G. Bultrini, G. M Ingo, *Archaeometry* **2001**, *43*, 529.

[13] D. A. Scott, *J. Am. Ite. Cons*. **1994**, *33*, 1.

[14] I. Constantinides, A. Adriaens, F. Adams, *Appl. Surf. Sci*. **2002**, *189*, 90.

[15] L. Robbiola, R. Portier, *J. Cult. Herit*. **2006**, *7*. 1.

[16] I. Sandu, C. Marutoiu, I. G. Sandu, A. Alexandru, A. V. Sandu, *Acta Universitatis Cibinensis Section F Chemia* **2006**, *9*, 39.

[17] L. Robbiola, J. -M. Blengino, C. Fiaud, *Corr. Sci*. **1998**, *40*, 2083.

[18] L. Robbiola, L. -P. Hurtel, Standard nature of the passive layers of buried archaeological bronze - The example of two Roman half-length portraits, in I.

MacLeod, S. Pennec, L. Robbiola, Eds., *METAL 95*, James & James Science Publ., London, 1997, pp. 109–117.

[19] F. Scholz, B. Meyer, Voltammetry of solid microparticles immobilized on electrode surfaces, *Electroanalytical Chemistry, A Series of Advances*, Bard, A. J., and Rubinstein, I., Eds., Marcel Dekker, New York, 1998, vol. 20, pp. 1–86.

[20] F. Scholz, U. Schröder, R. Gulabowski, A. Doménech-Carbó, *Electrochemistry of Immobilized Particles and Droplets*, 2nd edit. Springer, Berlin-Heidelberg, 2014.

[21] A. Doménech-Carbó, J. Labuda, F. Scholz, *Pure Appl. Chem*. **2013**, *85*, 609.

[22] A. Doménech-Carbó, M. T. Doménech-Carbó, V. Costa, *Electrochemical Methods in Archaeometry, Conservation and Restoration*, Monographs in Electrochemistry Series, F. Scholz, Edit. Springer, Berlin-Heidelberg, 2009.

[23] A. Doménech-Carbó, Tracing, authentifying and dating archaeological metal using the voltammetry of microparticles. *Anal. Methods* **2011**, *3*, 2181.

[24] A. Doménech-Carbó, M. T. Doménech-Carbó, *Pure Appl. Chem.* **2018**, *90*, 447.

[25] V. Costa, K. Leyssens, A. Adriaens, N. Richard, F. Scholz, *J. Solid State Electrochem*. **2010**, *14*, 449.

[26] F. Arjmand, A. Adriaens, *J. Solid State Electrochem*. **2012**, *16*, 535.

[27] N. Souissi, L. Bousselmi, S. Khosrof, E. Triki, *Mater. Corros*. **2004**, *55*, 284.

[28] Ottenwelter, E., V. Costa, *Archaeometry* **2015**, *57*, 497.

[29] A. Doménech-Carbó, M. T. Doménech-Carbó, I. Martínez-Lázaro, *Microchim. Acta* **2008**, *162*, 351.

[30] D. Satovic, S. Martinez, A. Bobrowski, *Talanta* **2010**, *81*, 1760.

[31] A. Doménech-Carbó, M. T. Doménech-Carbó, J. Redondo-Marugán, L. Osete-Cortina, M. V. Vivancos-Ramón, *Electroanalysis* **2016**, *28*, 833.

[32] D. Blum, W. Leyffer, R. Holze, *Electroanalysis* **1996**, *8*, 296.

[33] A. Doménech-Carbó, M. T. Doménech-Carbó, M. A. Peiró-Ronda, *Electroanalysis* **2011**, *23*, 1391.

[34] A. Doménech-Carbó, M. Lastras, F. Rodríguez, L. Osete-Cortina, *Microchem. J.* **2013**, *106*, 41.

[35] A. Doménech-Carbó, M. T. Doménech-Carbó, I. Martínez-Lázaro, *Anal. Chim. Acta* **2010**, *610*, 1.

[36] A. Doménech-Carbó, M. T. Doménech-Carbó, M. A. Peiró-Ronda, L. Osete-Cortina, *Archaeometry* **2011**, *53*, 1193.

[37] A. Doménech-Carbó, M. T. Doménech-Carbó, M. Lastras, M. Herrero, *For. Sci. Int.* **2015**, *247*, 79.

[38] A. Doménech-Carbó, M. T. Doménech-Carbó, M. A. Peiró-Ronda, *Anal. Chem.* **2011**, *83*, 5639.

[39] A. Doménech-Carbó, M. T. Doménech-Carbó, S. Capelo, T. Pasíes-Oviedo, I. Martínez-Lázaro, *Angew. Chem. Int. Ed.* **2014**, *53*, 9262.

[40] A. Doménech-Carbó, F. Scholz, M. T. Doménech-Carbó, J. Piquero-Cilla, N. Montoya, T. Pasíes-Oviedo, M. Gozalbes, M. Melchor-Monserrat, A. Oliver, *ChemElectroChem* **2018**, *5*, 2113.

[41] A. Doménech-Carbó, M. T. Doménech-Carbó, J. Redondo-Marugán, L. osete-Cortina, J. Barrio, A. Fuentes, M. V. Vivancos-Ramón, W. Al-Sekhaneh, B. Martínez, I. Martínez-Lázaro, T. pasíes-Oviedo, *Archaeometry* **2018**, *60*, 308.

[42] A. Doménech-Carbó, M. T. Doménech-Carbó, E. Montagna, Y. Lee, *Talanta* **2017**, *169*, 50.

[43] F. Di Turo, N. Montoya, J. Piquero-Cilla, C. De Vito, F. Coletti, G. Favero, M. T. Doménech-Carbó, A. Doménech-Carbó, *Electroanalysis* **2018**, *30*, 361.

[44] A. Doménech-Carbó, M. T. Doménech-Carbó, C. Álvarez-Romero, N. Montoya, T. Pasíes-Oviedo, M. Buendía, *Electroanalysis* **2017**, *29*, 2008.

[45] P. P. Ripollés, J. M. Abascal, *Saguntum* **1995**, *29*, 131.

[46] J. M. Abascal, P. P. Ripollés, M. Gozalbes, *Acta Numismatica* **1996**, *26*, 17.

[47] P. P. Ripollés, J. M. Abascal, *Acta Numismatica* **1998**, *28*, 33.

[48] C. Domergue, *Les mines de la Péninsule Ibérique dans l'Antiquité romaine*. Roma, 1990.

[49] D. Pavlov, B. Monakhov, *J. Electrochem. Soc.* **1989**, *136*, 27.

[50] W. –B. Cai, Y. –Q. Wan, H. –T. Liu, W. –F. Zhou, *J. Electroanal. Chem.* **1995**, *387*, 95.

[51] N. D. Meeks, *Archaeometry* **1986**, *28*, 133.

[52] C. Chiavari, K. Rahmouni, H. Takenouti, S. Joiret, P. Vermaut L. Robbiola, *Electrochim. Acta* **2007**, 52, 7760.

[53] M. Serghini-Idrissi, M. C. Bernard, F. Z. Harrif, S. Joiret, K. Rahmouni, A. Srhiri, H. Takenouti, V. Vivier, M. Ziani, *Electrochim. Acta* **2005**, *50*, 4699.

[54] V. Bongiorno, S. Campodonico, R. Caffara, P. Piccardo, M. M. Carnasciali, *J. Raman Spectrosc*. **2012**, *43*, 1617.

[55] E. Basso, C. Invernizzi, M. Malagodi, M. F. La Russa, D. Bersani, P. P. Lottici, *J. Raman Spectrosc*. **2014**, *45*, 238.

[56] W. T. Chase, Chinese bronzes: casting, finishing, patination and corrosion, in: D. A. Scott, J. Podany, B. Consodine, Eds. *Ancient, Historic Metals*. The Getty Conservation Institute, London, 1994, pp. 86–117.

[57] G. M. Ingo, P. Plescia, E. Angelini, C. Riccucci, T. De Caro, *Applied Physics A*, **2006**, *83*, 611.

Figures

Figure 1. Square wave voltammograms of samples from coins a,b) 41593 (Obulco), and c,d) 41540 (Cástulo), attached to graphite electrodes immersed into air-saturated 0.25 M HAc/NaAc at pH 4.75. Potential scan initiated at a,c) 0.65 V in the negative direction; b,d) −1.05 V in the positive direction; potential step increment 4 mV; square wave amplitude 25 mV; frequency 5 Hz. Dotted lines represent the base lines for peak current measurements. Insets: photographic images of the coins.

Figure 2. Detail of the region between 0.0 and −1.20 V of square wave voltammograms of microparticulate deposits of a) cuprite plus tenorite (50% wt); b) cuprite plus litharge (25% wt); c) cuprite (40% wt) plus tenorite (40% wt) plus litharge (20% wt) mixtures attached to graphite electrodes immersed into air-saturated 0.25 M HAc/NaAc at pH 4.75. Potential scan initiated at a,c) 0.65 V in the negative direction; b,d) −1.05 V in the positive direction; potential step increment 4 mV; square wave amplitude 25 mV; frequency 5 Hz.

Figure 3. Tentative schemes for the structure and composition of the patinas of a) binary Cu-Sn and b) ternary Cu-Sn-Pb bronze alloys.

Figure 4. Two-dimensional diagrams containing the mass percentages of: a) Cu vs. Pb, and b) Sn vs. Pb in double logarithmic scale, in the bulk alloy of Iberian coins reported by Ripollés et al. [45-47]. Solid rhombs: Iltirta and Ilerda coins; solid squares: Cástulo coins; triangles: Obulco coins. The arrows in b) mark the Cástulo and Obulco coins possessing high Sn loadings.

Figure 5. Separated plots of the the $i_p(C_2)/i_p(C_1)$ peak current ratio vs. $i_p(C_2)$ for coins from the Iltirta, Cástulo and Obulco mints in this study. Two or three spots for each coin are depicted.

Figure 6. Plots of $i_p(A_2)$ vs. $i_p(C_2)$ from voltammograms of particulate deposits from the corrosion layers of the studied Iberian coins. Conditions such as in Figure 1.

Figure 7. FESEM-FIB of coins a) 42127 (Iltirta); b) 41868 (Iltirta); c) 25654 (Cástulo); d) 25671 (Obulco). Secondary electron images recorded in trenches of *ca.* 10 μm length and *ca.* 15 μm depth generated by FIB in the region of interest in the coins.

Figure 8. Distribution of frequencies of the $i_p(A_2)/i_p(A_1)$ ratio values for a) Iltirta and b) Cástulo plus Obulco coins in this study. N_{coins} denote the number of replicate measurements displaying a $i_p(A_2)/i_p(A_1)$ value between the ratios indicated in the x-axis.

Figure 9. Variation of the $i_p(C_2)/i_p(C_1)$ peak current ratio on $i_p(C_2)$ for coins from the Iltirta mint in this study. Two or three spots for each coin are depicted. Continuous lines correspond to the fit of such sub-series of data to a potential law. The arrow indicates the growth of the lead corrosion products to copper corrosion products.

Figure 10. Variation of the $i_p(C_2)/i_p(C_1)$ peak current ratio on $i_p(C_2)$ for coins from the mints of Cástulo and Obulco in this study. Two or three spots for each coin are depicted. Continuous lines correspond to the fit of such sub-series of data to a potential law. The arrow indicates the growth of the lead corrosion products to copper corrosion products.

Figure 11. Tentative evolutive scheme for the minting in the Iberic cities of Iltirta, Cástulo and Obulco derived from electrochemical data. See text in section 3.5.

Figure 1.

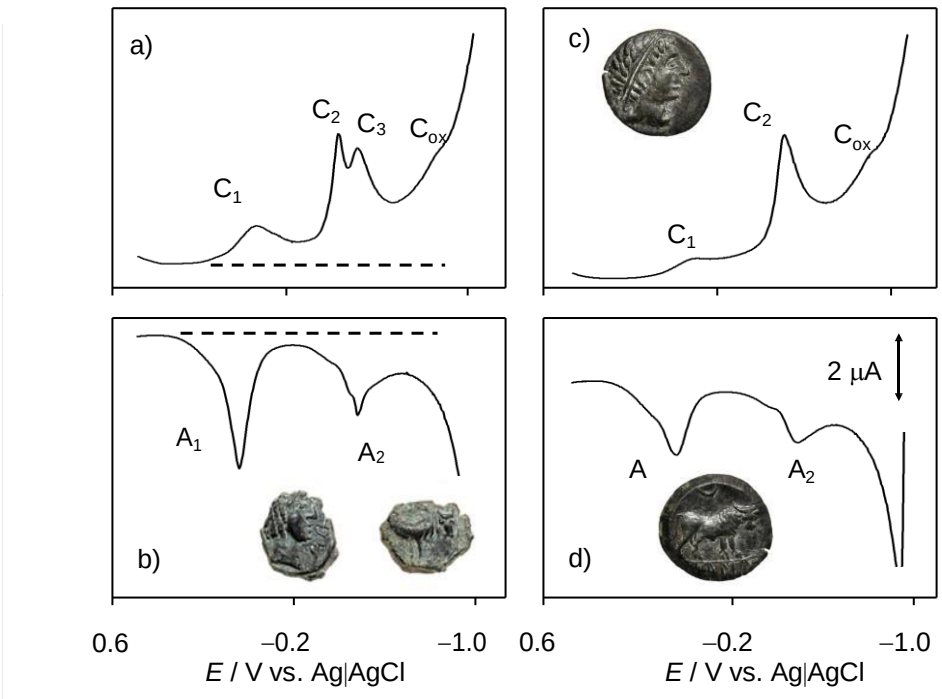
a)
C1
C2
C3
Cox
c)
C1
C2
Cox
b)
A1
A2
d)
2 μA
A
A2
0.6
–0.2
–1.0
E / V vs. Ag|AgCl
0.6
–0.2
–1.0
E / V vs. Ag|AgCl

Figure 2.

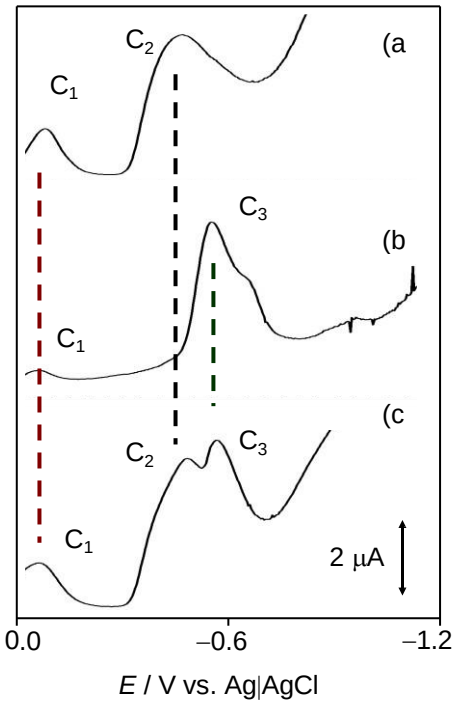

Figure 3.

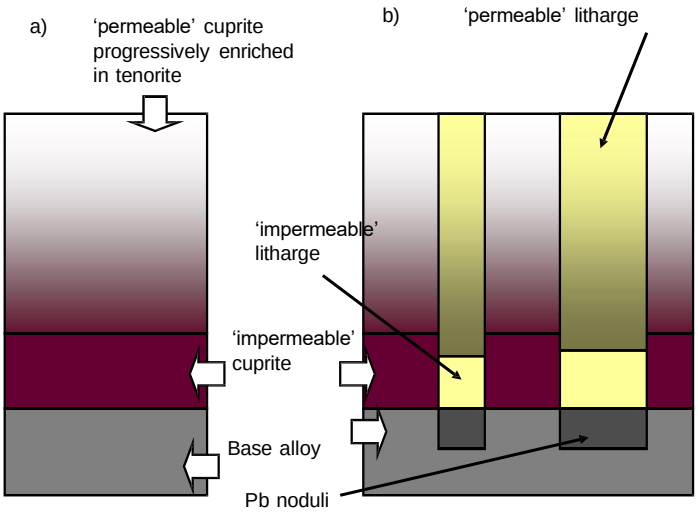
a)
'permeable' cuprite progressively enriched in tenorite
b)
'permeable' litharge
'impermeable' litharge
'impermeable' cuprite
Base alloy
Pb noduli

Figure 4.

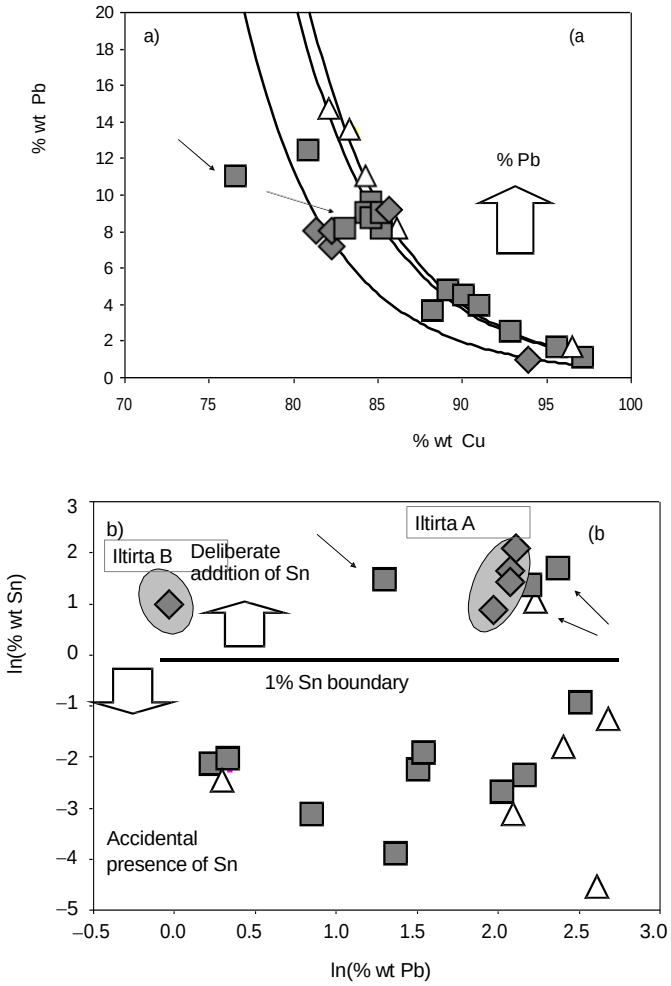
a)
(a
% wt Pb
% Pb
% wt Cu
b)
Iltirta A
(b
Iltirta B
Deliberate
addition of Sn
1% Sn boundary
Accidental
presence of Sn
ln(% wt Sn)
ln(% wt Pb)

Figure 5.

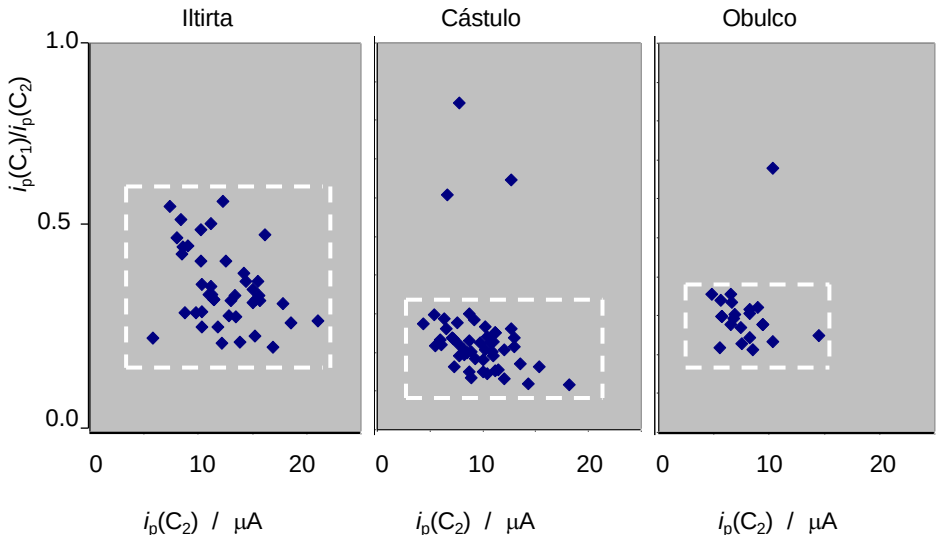

Figure 6.

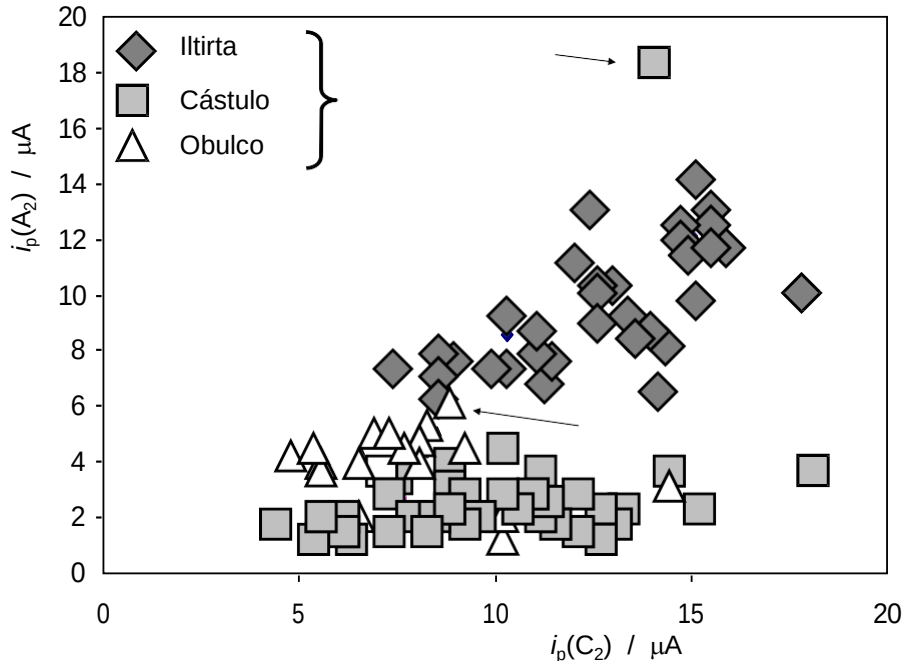
Iltirta
Cástulo
Obulco
$i_p(A_2)$ / μA
$i_p(C_2)$ / μA
0
2
4
6
8
10
12
14
16
18
20
0
5
10
15
20

Figure 7.

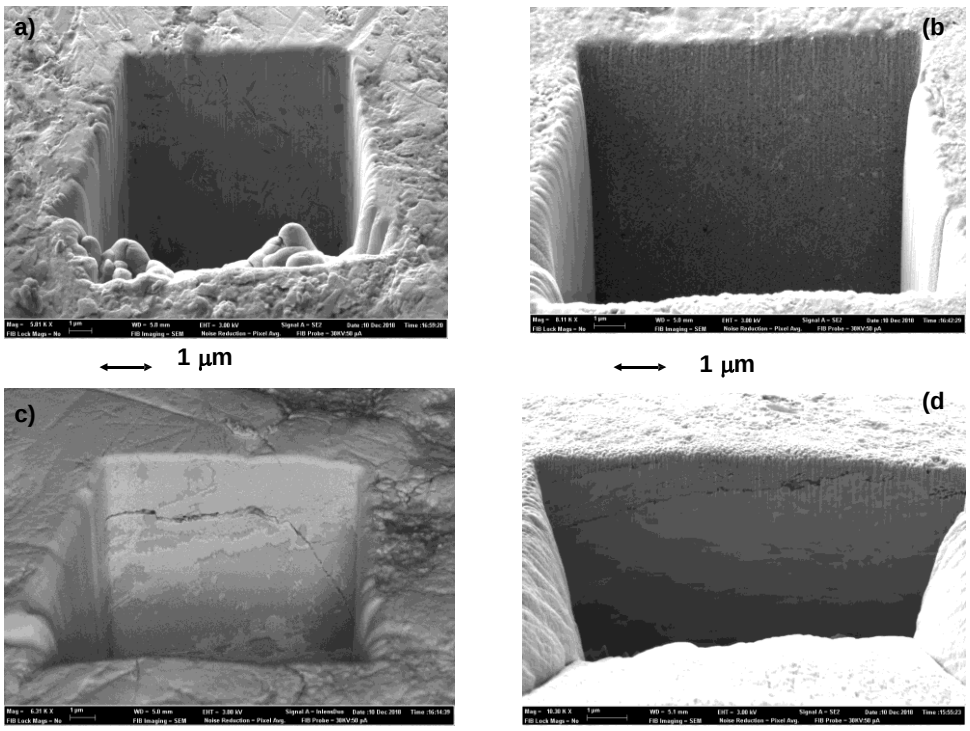

Figure 8.

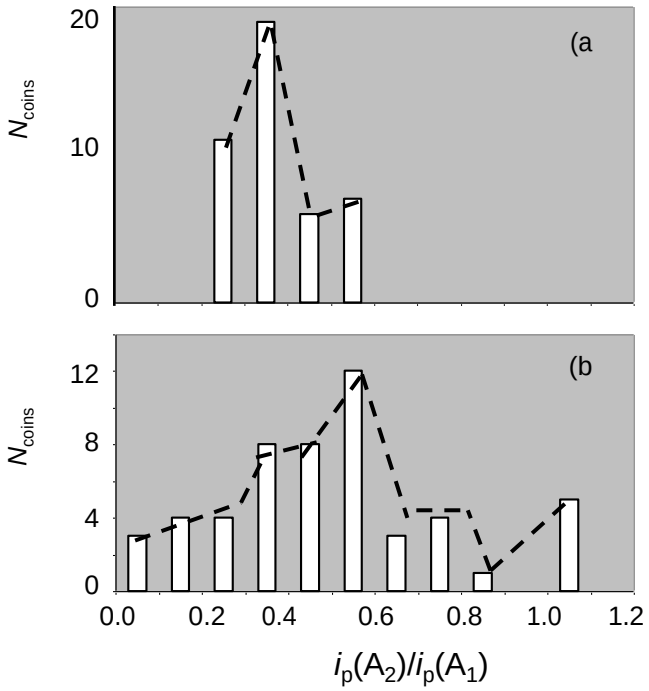

Figure 9.

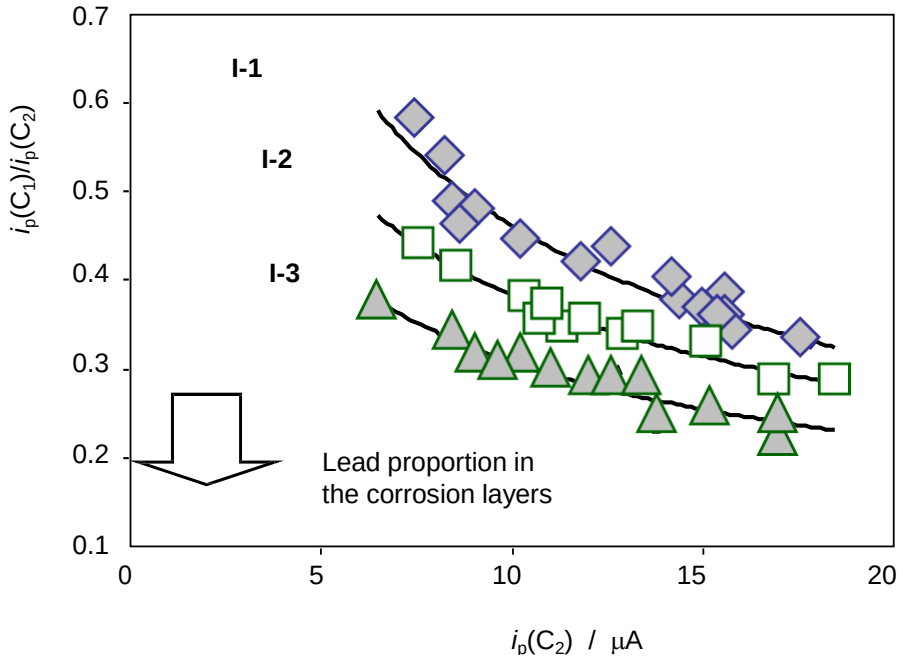
0.7
0.6
0.5
0.4
0.3
0.2
0.1
0
5
10
15
20
I-1
I-2
I-3
Lead proportion in
the corrosion layers
$i_p(C_1)/i_p(C_2)$
$i_p(C_2)$ / μA

Figure 10.

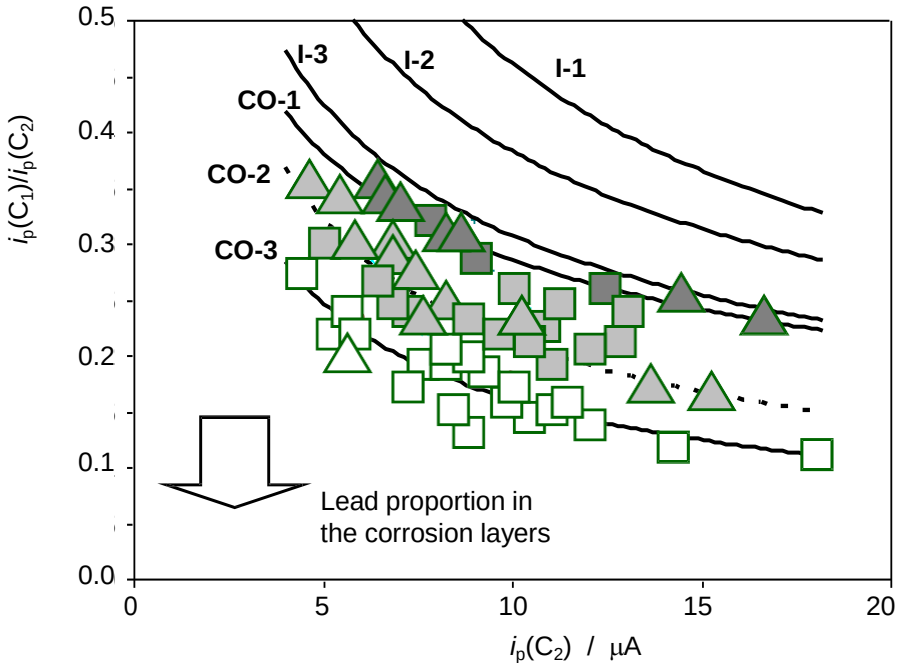
0.5
0.4
0.3
0.2
0.1
0.0
0
5
10
15
20
$i_p(C_1)/i_p(C_2)$
$i_p(C_2)$ / μA
I-3
I-2
I-1
CO-1
CO-2
CO-3
Lead proportion in
the corrosion layers

Figure 11.

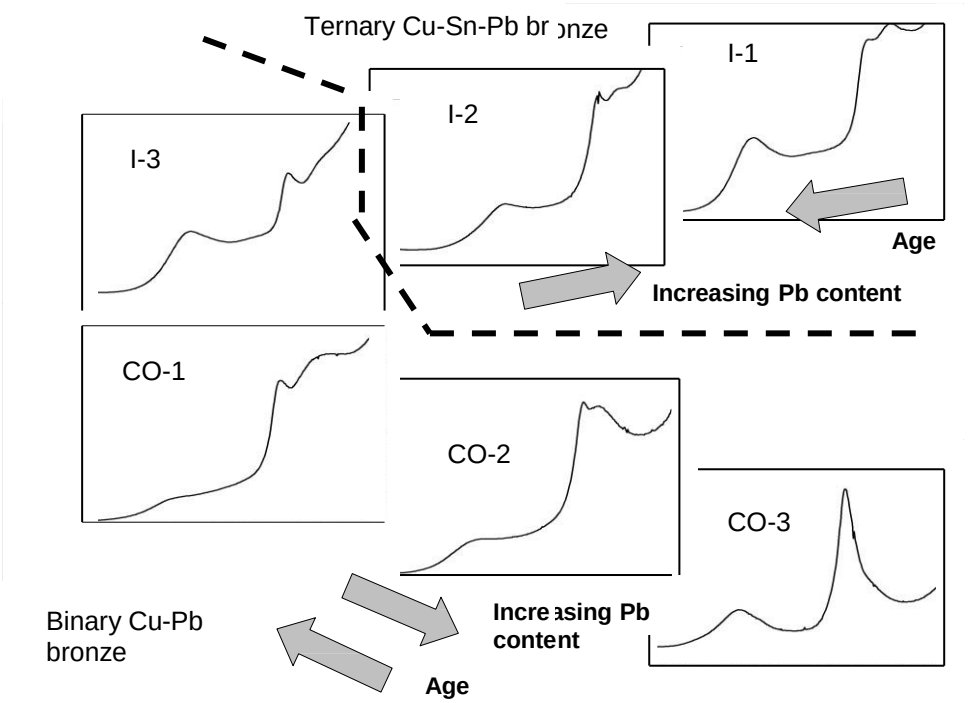
Ternary Cu-Sn-Pb br onze
I-1
I-2
I-3
Age
Increasing Pb content
CO-1
CO-2
CO-3
Binary Cu-Pb bronze
Incre asing Pb content
Age